

SCIENTIFIC REPORTS



OPEN

Exploring the topological sources of robustness against invasion in biological and technological networks

Fernando Alcalde Cuesta^{1,2}, Pablo González Sequeiros^{1,3} & Álvaro Lozano Rojo^{1,4,5}

Received: 06 November 2015

Accepted: 11 January 2016

Published: 10 February 2016

For a network, the accomplishment of its functions despite perturbations is called robustness. Although this property has been extensively studied, in most cases, the network is modified by removing nodes. In our approach, it is no longer perturbed by site percolation, but evolves after site invasion. The process transforming resident/healthy nodes into invader/mutant/diseased nodes is described by the Moran model. We explore the sources of robustness (or its counterpart, the propensity to spread favourable innovations) of the US high-voltage power grid network, the Internet2 academic network, and the *C. elegans* connectome. We compare them to three modular and non-modular benchmark networks, and samples of one thousand random networks with the same degree distribution. It is found that, contrary to what happens with networks of small order, fixation probability and robustness are poorly correlated with most of standard statistics, but they depend strongly on the degree distribution. While community detection techniques are able to detect the existence of a central core in Internet2, they are not effective in detecting hierarchical structures whose topological complexity arises from the repetition of a few rules. Box counting dimension and Rent's rule are applied to show a subtle trade-off between topological and wiring complexity.

A biological or technological system is *robust* if it continues to function despite perturbations. Different names have been used for this concept depending on the nature of the system, the particular feature to be considered robust, and the kind of change to be applied. *Scale-free networks*¹ have been proposed as models of complex networks enjoying an unexpected degree of *robustness* or *error tolerance* when a fraction of nodes is removed at random. The World-Wide-Web, the Internet and several social networks have been regarded as interesting examples by many authors. However, these real networks seem extremely vulnerable to targeted attacks on the highly connected nodes. Similar conclusions were stated for living systems like metabolic networks² and PPI networks³ after computational removal of randomly chosen nodes. These results suggest an evolutionary selection of the topological structure of biological networks in both senses, global generating mechanisms that give rise to power laws, as local correlating degree connectivity and influence in the network.

To understand the paradoxical “robust yet fragile” nature of all these networks, other scenarios have been also explored. *Highly Optimised Tolerance (HOT) models*⁴ were proposed from the double perspective of the existence of technological and economical constraints limiting the network topology and the accomplishment of their functional objectives. Abilene, the backbone for the Internet2 academic network, was used to illustrate the performance of this kind of models after node removal⁴.

Our aim was to explore the topological sources of another kind of robustness of biological and technological networks. In our approach, such a network is no longer perturbed by site percolation, but it evolves after the attack of pathogens like viruses or prions. The evolutionary process transforming *healthy* (or *resident*) nodes into *diseased* (or *invader*) nodes is described by the Moran model on networks introduced by Lieberman *et al.*⁵.

¹GeoDynApp - ECSING Group (Spain). ²Instituto de Matemáticas, Universidade de Santiago de Compostela, E-15782 Santiago de Compostela (Spain). ³Departamento de Didáctica das Ciencias Experimentais, Facultade de Formación do Profesorado, Universidade de Santiago de Compostela, Avda. Ramón Ferreiro 10, E-27002 Lugo (Spain). ⁴Centro Universitario de la Defensa Zaragoza, AGM, Ctra. Huesca s/n. E-50090 Zaragoza (Spain). ⁵Instituto Universitario de Matemáticas y Aplicaciones, Universidad de Zaragoza (Spain). Correspondence and requests for materials should be addressed to A.L.R. (email: alvarolozano@unizar.es)

Morbidity depends on the relative *fitness* of the pathogen with respect to the immune answer of healthy nodes. More precisely, at the beginning, all nodes are healthy. Then, one node chosen at random becomes infected by the pathogen. At successive steps, a diseased or healthy node is chosen at random with probability proportional to the relative fitness $r \geq 1$ or $r = 1$. Next, a randomly chosen neighbour of the node is infected or cured. The (*average*) *fixation probability* is the probability that all the nodes of the network become infected. For a homogeneous or well-mixed networks this invasion process coincides with the classical Moran process⁶. In fact, *isothermal networks* has the same fixation probability that the homogeneous networks⁵. However, there are networks structures acting like evolutionary amplifiers favouring the disease spread across the network^{5,7–9}.

In this context, we called *robustness against invasion* to a measure of the proximity of the network to the isothermal equilibrium. Here, we attempted to explore the topological sources of this kind of pathogen tolerance or its counterpart, the propensity to spread favourable innovations¹⁰. Therefore, motivated by the aforementioned works about usual robustness, we studied the robustness against invasion of the *US Power Grid (PG)*¹¹ and *Internet2 (I2)* technological networks, and the neuronal network of the hermaphrodite nematode *Caenorhabditis elegans (CE)*^{12,13}, see Data.

On the other hand, many researchers are interested in modularity and hierarchical modularity of technological and biological networks^{14–20}, searching for adaptive, spatial, or economical constraints on their evolution^{4,21–23}. According to them, modular architecture allows a faster adaptation to environmental changes, and their robustness is a major advantage when networks evolve under natural selection. Thus, we added a *hierarchical modular network (HR)*²⁰ and a *random toy model (TW)*²¹ to contrast modularity and to test spatial aggregation propensity. Modular networks have the property of small-worldness²⁴ characterised by a relative short average path length and a high clustering coefficient, favouring a low wiring cost. However, there are small-world networks that are not modular, so we also added the scale-free *Barabási-Albert model (BA)*²⁵ to our study.

We computed the fixation probability using the Monte Carlo method on the associated Embedded Markov Chain, called the *EMC method*⁷. This allowed us to estimate the robustness against invasion of these networks. In an effort to understanding the structural causes of this robustness, we compared the fixation probability of the four deterministic networks PG, I2, CE and HR to that of samples of 10^3 random networks having the same degree distribution.

Results

Mathematical model. Consider an undirected connected network $G = (V, E)$ with node set $V = \{1, \dots, N\}$ with no loops or multiple edges. Denote by d_i the degree of the node i . The *Moran process* on G with fitness r is the following Markov chain: start with a population V of N healthy nodes. Afterward, one single node i_0 is chosen, with probability $1/N$, to become a diseased node. At successive steps one node i is selected at random with probability $r_i/(N - m + rm)$, where r_i is 1 or r depending on whether i is healthy or diseased, and m is the number of diseased nodes in that moment. Next, a neighbour of i , randomly chosen with probability $1/d_i$, becomes healthy or diseased depending on whether i is healthy or diseased. The *fixation probability*, denoted $\Phi(r)$, is the probability that the whole population becomes diseased at some time step. For more details, see Supplementary Information.

Fixation function and robustness. The computation of the fixation probability leads to a system of 2^N equations, see Supplementary Information. Hence, except where global or partial symmetries reduce the number of equations^{5,7}, analytically solving the system is infeasible if the order of the network is not a very small. Thus, we computed the fixation probability of the three real networks PG, I2 and CE and the deterministic hierarchical one HR applying the EMC method⁷ and using 10^5 trials and fitness values r varying from 0 to 10 with step size of 0.25. Each of these fixation functions is compared with the exact and asymptotic fixation functions $\Phi_0(r)$ and $\Phi_2(r)$ for equivalent sized complete and complete bipartite networks, which are given in Methods, Equations (2) and (3) respectively. Each of these fixation functions was also compared to the fixation function on average from a benchmark sample of 10^3 networks having the same degree distribution. Graphical representations of these fixation functions in Fig. 1 show a strong dependence on the degree distribution, which indeed increases for the most robust networks CE and HR. We repeated the computation for the random networks BA and TW, which also are robust networks.

To give a more accurate measure of the robustness of these networks, we introduce the *robustness against invasion*

$$\rho = \frac{1}{1 + \|\Phi - \Phi_0\|_\infty / \|\Phi_2 - \Phi_0\|_\infty} = \frac{\|\Phi_2 - \Phi_0\|_\infty}{\|\Phi_2 - \Phi_0\|_\infty + \|\Phi - \Phi_0\|_\infty}. \quad (1)$$

For details see Methods. We estimated the value of ρ approximating $\|\Phi - \Phi_0\|_\infty$ and $\|\Phi_2 - \Phi_0\|_\infty$ by the supremum of the differences $|\Phi(r) - \Phi_0(r)|$ and $|\Phi_2(r) - \Phi_0(r)|$ where r varies from 1.25 to 10 with steps of size 0.25. The data is shown in Table 1, which includes both average and standard deviation of ρ for random or randomised networks.

Heterogeneity. The notions of *heterogeneity*^{26,27} and *heat heterogeneity*¹⁰ (i.e. the variance of degree and temperature respectively) were proposed as strong indicators of the fixation probability for some small networks. We compared both heterogeneities with the fixation probability in the neutral case $r = 1$ and in the non-neutral case $r = 1.25, 1.5, 1.75, 2$. The most interesting cases $r = 1$ and $r = 1.5$ are shown in Fig. 2. The rest of the cases are similar to $r = 1.5$, see Supplementary Information.

For the networks considered here, both heterogeneity and heat heterogeneity show a poor correlation with $\Phi(1.5)$, see Table 1 and Fig. 2. In fact, Kendall's rank correlation coefficient values $\tau = -0.33$ for H_d and $\tau = 0.38$

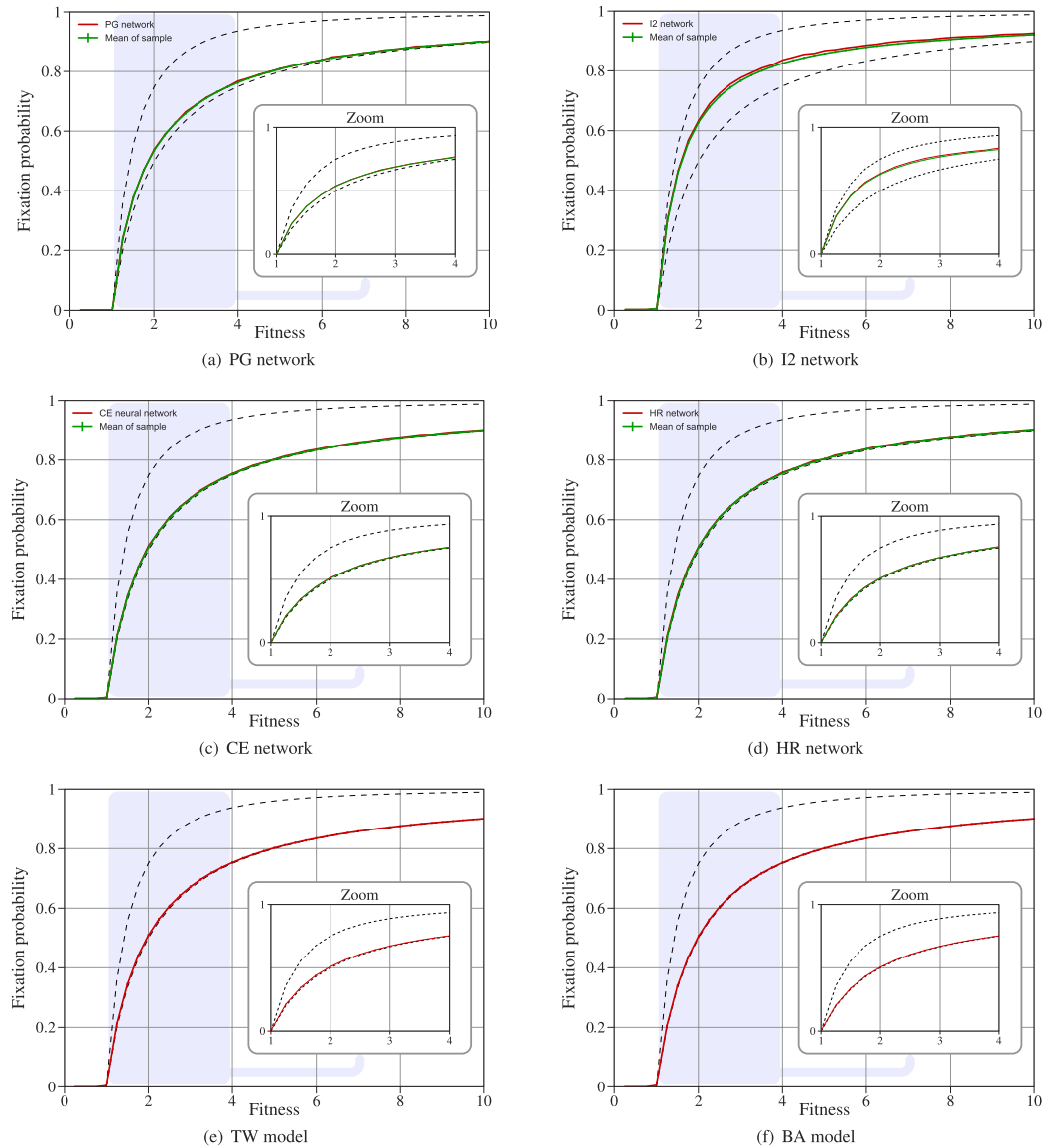


Figure 1. (a–d) Fixation probability functions for the US Power Grid, Internet2, *C. elegans* neuronal and hierarchical HR networks and asymptotically uniform samples of 10^5 networks with the same degree distributions. We used 10^5 and 10^4 trials respectively for every fitness value r varying from 0 to 10 with step size of 0.25. (e–f) Fixation probability functions for the Toy Worm and Barabási-Albert random models with samples of 10^3 networks and 10^4 trials for the same values of r .

for H_r . Figs 1 and 2 support the idea that robustness and fixation probability depend strongly on the degree distribution. So it is natural to study the correlation of the fixation probability in both neutral and non-neutral cases with other statistics directly related with the degree distribution such as *mean degree* (δ), *degree median* (q_2), *degree skewness* and *degree kurtosis*, the network's global scale such as *size* (N), *edge number*, *diameter* and *temperature entropy* (I_t), or the network's topology such *clustering coefficient* (C), *transitivity ratio*, *average path length* (L), *power law exponent*, *Q-modularity*, *I-modularity* and *fractal dimension* (D). The values of these statistics are shown in Tables 1 and 2.

We concluded that N and I_t are the best correlated quantities with the fixation probability in the neutral case $r = 1$, with $\tau = -0.91$ (having mutual Kendall's $\tau = 1$). In the non-neutral case $r = 1.5$ the most correlated statistics are the median degree with $\tau = -0.77$, the mean degree with $\tau = -0.74$, and the average path length L with $\tau = 0.56$, together with N and I_t having $\tau = 0.58$, see Table 3. Nevertheless, at least for the networks considered here, robustness is moderately well correlated with the median degree with $\tau = 0.86$, the mean degree δ with $\tau = 0.83$ and the ratio C/L with $\tau = 0.69$, but it is rather poorly correlated with the other basic statistics. But it is reasonable to think that the correlations with the median and mean degree are biased by the nature of the considered networks, see Discussion.

Network	ρ	$\Phi(1.5)$	δ	H_d	H_t	C	L	C/L
BA	0.954 ± 0.010	0.339 ± 0.005	19.00	12.14 ± 0.37	0.48 ± 0.04	0.18 ± 0.01	2.06 ± 0.01	0.089 ± 0.004
CE	0.948	0.345	16.39	12.49	0.88	0.34	2.44	0.138
HR	0.946	0.348	6.87	12.69	6.12	0.59	2.41	0.246
HR random	0.942 ± 0.010	0.341 ± 0.005	6.87	12.69	5.53 ± 0.07	0.25 ± 0.01	2.33 ± 0.01	0.108 ± 0.003
CE random	0.942 ± 0.011	0.344 ± 0.005	16.39	12.49	0.74 ± 0.03	0.14 ± 0.00	2.27 ± 0.01	0.062 ± 0.002
TW	0.940 ± 0.012	0.344 ± 0.005	4.75 ± 0.15	1.83 ± 0.09	0.18 ± 0.02	0.24 ± 0.02	6.51 ± 0.18	0.037 ± 0.003
PG	0.855	0.376	2.67	1.79	0.74	0.08	18.99	0.004
PG random	0.845 ± 0.010	0.377 ± 0.005	2.67	1.79	0.65 ± 0.01	0.00 ± 0.00	8.71 ± 0.03	0.000 ± 0.000
I2 random	0.649 ± 0.007	0.460 ± 0.005	2.08	3.06	6.07 ± 0.23	0.00 ± 0.00	5.63 ± 0.26	0.000 ± 0.000
I2	0.639	0.464	2.08	3.06	7.38	0.00	8.26	0.000

Table 1. Robustness and fixation probability in the non-neutral case $r = 1.5$ compared with mean degree δ , heterogeneity H_d , heat heterogeneity H_t and some small-worldness measures (on average for asymptotically uniform samples of 10^3 networks in random networks). Networks are sorted by robustness.

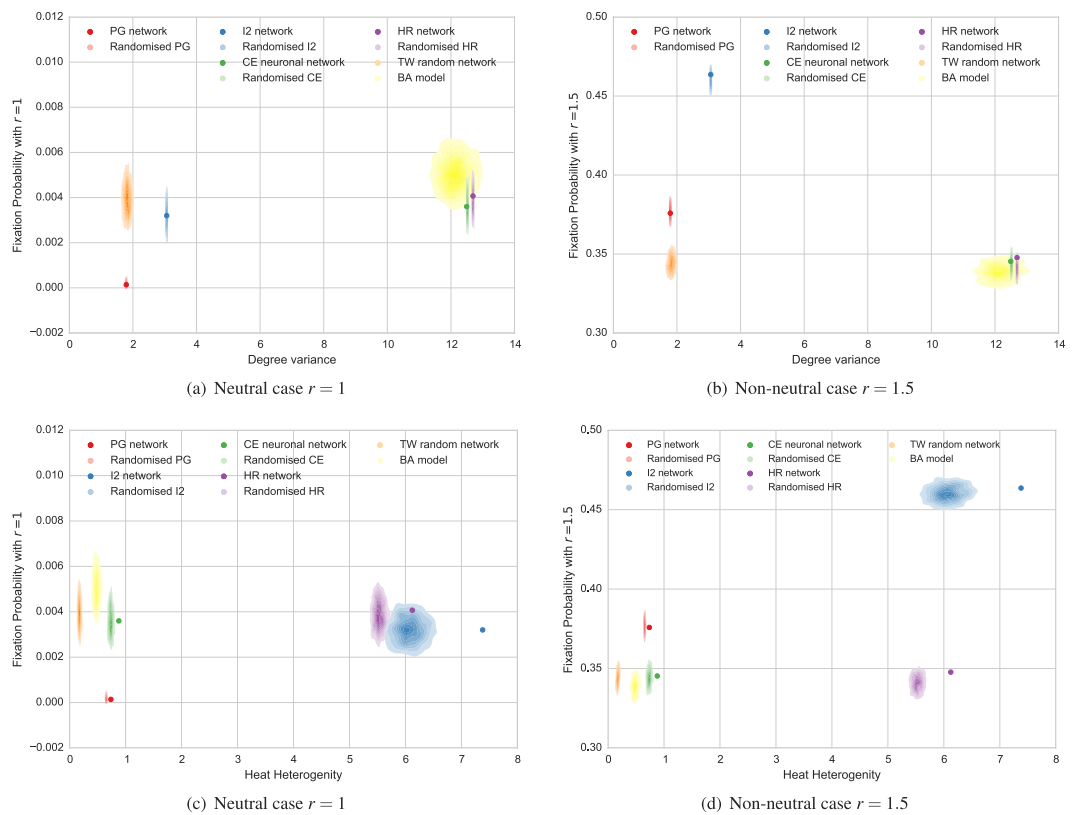


Figure 2. Comparing fixation probability in the neutral and non-neutral case with (a,b) variance of the degree distribution and, (c,d) heat heterogeneity¹⁰.

Modularity and hierarchical modularity. For many years, researchers have been interested in modularity and hierarchical modularity, searching for dynamic and evolutionary constraints that justify why biological and technological networks have a modular architecture. We were initially interested in two types of modularity. In the first one, the network splits into densely connected modules which are sparsely interconnected. The second one uses the idea that modular architecture reduces the information flow between modules.

Thus, we computed the Q -modularity²⁸, using *Louvain method* proposed by Blondel *et al.*²⁹. The results can be seen in Table 2, where Q is compared with the robustness ρ and the fixation probabilities $\Phi(1)$ and $\Phi(1.5)$, see also Fig. 3. For the networks considered here, the Q -modularity has positive Kendall's $\tau = 0.73$ with respect to the

Network	ρ	$\Phi(1)$	$\Phi(1.5)$	Q	I	D	std err	R	D'
BA	0.954 ± 0.010	0.005 ± 0.001	0.339 ± 0.005	0.17 ± 0.00	7.41 ± 0.01	6.22 ± 0.08	0.01	0.962	6.22
CE	0.948	0.004	0.345	0.40	7.49	4.26	0.18	0.995	4.26
HR	0.946	0.004	0.348	0.61	5.65	4.08	1.40	0.810	4.08
HR random	0.942 ± 0.010	0.004 ± 0.000	0.341 ± 0.005	0.31 ± 0.01	7.26 ± 0.02	4.95 ± 0.13	0.02	0.945	4.92
CE random	0.942 ± 0.011	0.004 ± 0.001	0.344 ± 0.005	0.20 ± 0.00	7.81 ± 0.00	5.20 ± 0.15	0.01	0.984	5.18
TW	0.940 ± 0.012	0.004 ± 0.001	0.344 ± 0.005	0.73 ± 0.01	5.40 ± 0.07	2.03 ± 0.06	0.00	0.979	2.02
PG	0.855	0.000	0.376	0.94	4.74	2.69	0.06	0.978	2.69
PG random	0.845 ± 0.010	0.000 ± 0.000	0.377 ± 0.005	0.75 ± 0.00	6.74 ± 0.01	3.21 ± 0.06	0.01	0.910	3.21
I2 random	0.649 ± 0.007	0.003 ± 0.001	0.460 ± 0.005	0.85 ± 0.00	3.60 ± 0.02	2.63 ± 0.15	0.00	0.976	2.58
I2	0.639	0.003	0.464	0.86	3.58	2.14	0.09	0.970	2.14

Table 2. Robustness and fixation probabilities compared with Q -modularity, I -modularity and fractal dimension, on average for asymptotically uniform samples of 10^3 networks in random networks. For fractal dimension we include the coefficient of determination R in the fit of the power law (7). For each random or randomised network, all the networks in the sample are considered at once, fitting the whole data set by a single regression line of slope D' . Differences between fractal dimension on average and exponent in a global fit are less than 0.05.

	q_2	δ	C/L	Q	I	C	D	N	I_t	L
ρ	0.86	0.83	0.69	-0.64	0.60	0.60	-0.56	-0.49	-0.49	-0.47
$\Phi(1)$	0.44	0.46	0.51	-0.56	0.24	0.51	0.29	-0.91	-0.91	-0.64
$\Phi(1.5)$	-0.77	-0.74	-0.42	0.73	-0.60	-0.33	-0.64	0.58	0.58	0.56

Table 3. Kendall's rank correlation coefficient for robustness and fixation probability in the neutral and non-neutral cases ($r = 1$ and $r = 1.5$) with respect some statistics sorted by their absolute values with respect to the robustness.

fixation probability in the non-neutral case $r = 1.5$ and negative $\tau = -0.64$ with respect to the robustness against invasion. The CE neuronal network shows a poor Q -modularity, $Q = 0.40$, but significantly higher than that of the corresponding randomised network, $Q = 0.20$. In general, Q -modularity is sensitive to the randomization process. The Q -modularity of the hierarchical HR network is moderate, $Q = 0.61$, contrary to what happens with the technological networks PG and I2 with a high Q -modularity and a central core or “hub subcomplex” in their structure.

We also adopted the point of view by Rosvall *et al.*^{30,31} replacing Q by the *Infomap code* or *minimum description length* I , see Table 2 and Fig. 3. For the networks considered here the correlations of I with the robustness ρ and the fixation probability $\Phi(1.5)$ are a little worse than those of Q . Both modularities has a mutual (negative) moderate correlation with $\tau = -0.69$, but they seem to have different nature according to the clustering in Fig. 4.

Community structure. The idea that high Q -modularity is correlated with the existence of a central core or “hub subcomplex” was explicitly tested on the Internet2 network and the hierarchical HR networks of level ≤ 4 . We used *Louvain algorithm*²⁹ to detect the community structure of these networks. For I2 network, it produces a similar but not identical community structure to the actual one, suggesting a more suitable placement of some connectors, see Supplementary Information. As counterpoint to the robustness, the spreading of favourable innovations can be enhanced by this kind of structures¹⁰ that incorporate trade-offs between performance and available resources⁴. Thus, community detection techniques could allow us to optimise the accomplishment of the functional objectives of a network with the same resources. However, these techniques are not equally effective in detecting other hierarchical modular structures, like the HR network, more topologically complex but constructed by repeating a simple rule, see Supplementary Information for details. Consequently, we say that a network is *repetitive* if it is obtained from the repetition of a reduced number of deterministic or random rules that encode its topological and dynamical complexity.

Topological complexity. Song *et al.* investigated the role of the fractal modular architecture in the robustness of some biological networks^{32,33}. But the renormalisation mechanism that characterises this architecture continues to operate in the non-fractal case: there are models and examples of real networks showing a fractal behaviour in small scales, although they behave globally as small-worlds. We have seen that the BA model, and the CE and HR networks are robust small-worlds, while the PG and I2 networks are modular networks with central cores. From the point of view of both small-worldness (measured by the ratio C/L) and modularity (measured by Q), the robust TW random model appears to be at an intermediate position. It has no central core because of the construction itself.

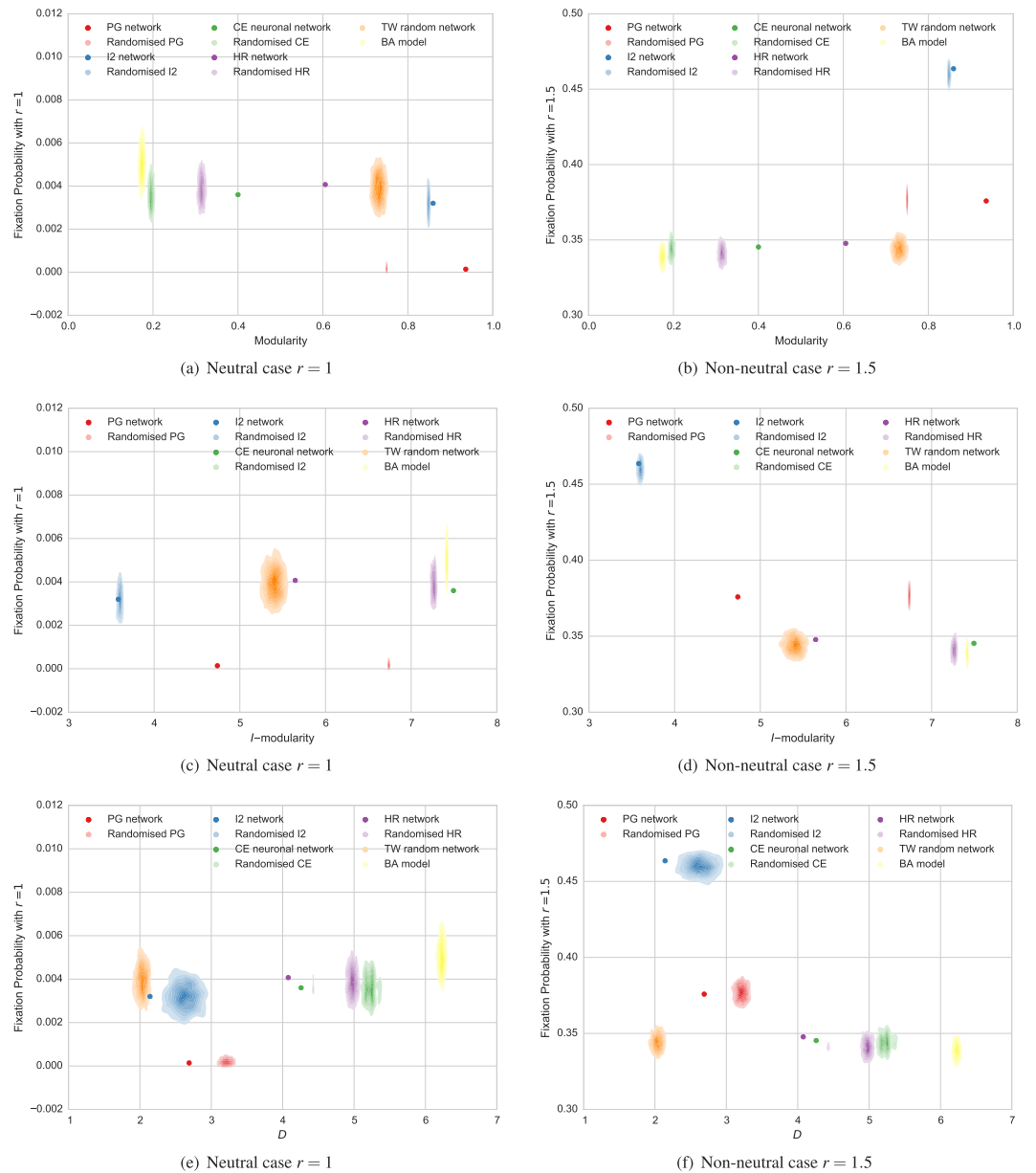


Figure 3. Comparing fixation probability in the neutral and non neutral cases with (a,b) Q-modularity, (c,d) I-modularity and, (e,f) fractal dimension.

Our computations of the fractal dimension D are consistent with the global picture sketched above, except for the random TW model which has the lowest fractal dimension. See Table 2. Like the over-representation of some motifs in both *C. elegans* neuronal¹⁸ and random TW²¹ networks, the robustness of both networks could be favoured by some kind of spatial aggregation. By its construction, TW has similar properties to the planar lattice, including its fractal dimension. There also might be spatial reasons for the properties of the *C. elegans* connectome, but obviously these cannot be the same as the given above.

Nevertheless, similarly to what happens with Rent's rule^{34–36} to analyse internal communications in integrated circuits, fractality measures could be perturbed by the existence of two regions in the log-log plots. Namely, a *Region I* where the linear scaling show a fractal topology, and a *Region II* where the scaling is not linear but exponential. By restriction to Region I, we obtained new estimates, but the new data do not alter the picture above. See Supplementary Material for these results.

Wiring complexity. In fact, Rent's rule has been applied to some biological networks including *C. elegans* connectome^{22,36,37}. Our estimates of Rent's exponents somewhat differ from those obtained by these authors. This is due to the different ways in which boxes decompositions are constructed, using box counting instead of min-cut partition algorithms. Values for the random TW ($p = 0.61$), the PG ($p = 0.64$) and the I2 ($p = 0.69$) networks belong to the range of values that requires a cost-efficient wiring architecture for VLSI circuits. But the HR

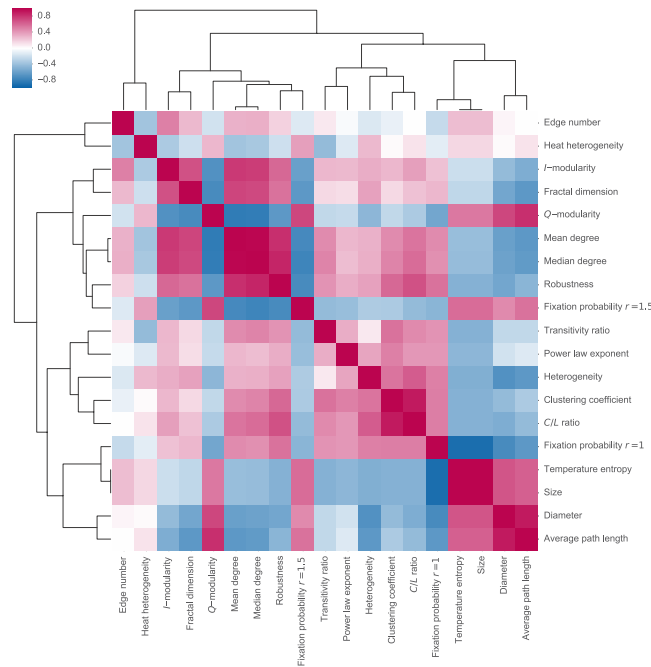


Figure 4. Comparing Kendall's correlation coefficients.

network has also a similar Rent's exponent ($p = 0.66$) showing that a high topological complexity is compatible with a moderate wiring complexity. On the contrary, the BA model and the CE connectome exhibit high interconnection complexity with Rent's exponents $p = 0.93$ and $p = 0.92$ respectively. In all cases, randomisation process increases Rent's exponents as well as the fractal dimension. Now, a combination of repetitiveness with some randomness, which is missing in the HR network, could justify a gain of topological and wiring complexity without affecting the robustness of network like the CE connectome.

Finally, Fig. 4 shows a global picture of the correlations. The hierarchical clustering of different statistics (with respect to the taxicab metric) is illustrated with a dendrogram. Most notable is the clustering of the modularity measures, in especial Q and D , around the robustness and the fixation probability in the non-neutral case $r = 1.5$.

Discussion

We computed the fixation functions for US Power Grid, Internet2 and *C. elegans* neuronal networks and asymptotically uniform samples of 10^3 randomly constructed networks with the same degree distributions. We completed these calculations with the fixation probability functions of four other benchmark networks: the hierarchical network constructed by Ravasz *et al.*²⁰, the corresponding randomised sample of 10^3 networks with the same degree distribution, the random toy model constructed by Artzy-Randrup *et al.*²¹ and the Barabási-Albert model²⁵, both with the same sample size as above. Moreover, we introduced the *robustness against invasion* to measure the proximity of a network to the isothermal equilibrium, that is, the equivalence of the network to a homogeneous population from the point of view of the Moran process. This quantity is interpreted as pathogen tolerance.

We distinguished two different groups: a first group of robust small-worlds formed by the BA model and the CE and HR networks with the corresponding randomised networks, and a second group of modular networks with central cores formed by PG and I2 with their corresponding randomised benchmarks. Regarding small-worldness and modularity, the TW model appears to be in an intermediate position. In the paper, we attempted to explore the topological sources of the robustness against invasion.

Initially, heterogeneity^{26,27} and heat heterogeneity¹⁰, defined as the variances of the degree and temperature distributions, were proposed as statistics well correlated with the fixation probability on some networks of small order. But neither heterogeneity, nor heat heterogeneity seem to have a determining effect on the fixation probability of these technological and biological large networks. In fact, we have shown that there is a strong dependence on the whole degree distribution. Consequently, it is not surprising that specific statistical correlations are not too high.

In the neutral case $r = 1$, we proved that the size and the temperature entropy⁸ are equally very well (negatively) correlated with the fixation probability $\Phi(1)$. In the non-neutral case $r = 1.5$, the median degree and the mean degree are also (negatively) well correlated to the fixation probability $\Phi(1.5)$, which now gives a measure of the propensity to spread favourable innovations¹⁰. With respect to the robustness ρ , the ratio C/L between the average path length L and the clustering coefficient C is also moderately correlated. But as evidenced by our own numerical experiments (to be published elsewhere), correlations with respect the median and mean degree are much lower on networks of small order.

Small-worldness of the *C. elegans* neuronal network was evidenced by other authors. In some cases, they used the same model as we did to describe the CE connectome¹⁵. In other cases, the model is similar, but not exactly the same^{12,22,23}, even if the data have been obtained at the same source¹³. Our estimations for $C = 0.34$ and $L = 2.44$ coincide with those given by Kim *et al.*¹⁵, except that we rounded up to 2 decimal places.

To precise the global picture of the biological and technological networks considered here, we also estimated the Q -modularity, the I -modularity and the fractal dimension of these networks. As explained in Methods, the Q -modularity was calculated by using the Louvain method proposed by Blondel *et al.*²⁹. In fact, the same method was already used by Basset *et al.*²² to estimate Q for the CE connectome obtaining the same low value $Q = 0.40$. On the other hand, using an older algorithm³⁸, Pan *et al.*²³ gave a slightly lower estimate $Q = 0.39$ where all the numbers are still rounded up to 2 decimal places. In fact, this authors make another estimate assuming that communities in CE connectome correspond to ganglia where $Q = 0.17$. The same approach (but using a different algorithm) was applied by Kim *et al.*¹⁵ obtaining a value $Q = 0.15$. Note however that these results could be biased by the edge/link swapping algorithm to randomise CE connectome. Regarding fractality, the use of the box counting method for networks with low diameter represents the main limitation, because these networks are rapidly covered by a single box. This applies to the BA model and the CE and HR networks, as well as their randomised benchmarks. In the particular case of the CE connectome, Bassett *et al.*²² used a standard partitioning algorithm to estimate what they call *topological fractal dimension* D_T . Explicitly, they obtained the value $D_T = 4.42$ which is higher than the box-counting dimension $D = 4.26$ and the box-counting dimension $D_I = 3.76$ in restriction to the Region I. Nevertheless, their results using the box-counting method coincide with ours, both included in the corresponding Supplementary Informations.

Our results are also consistent with previous observations correlating Q -modularity with the existence of a central core or “hub subcomplex” in the network, although one must be careful about interpreting the Q -modularity values obtained here: high for the technological networks PG and I2, both modular with central core, medium for HR and TW, and low for BA and CE. The idea that a high Q -modularity is correlated with the existence of this kind of core has been tested by describing explicitly the community structure of the Internet2 network and the HR networks of level ≤ 4 . While community detection techniques are able to identify the central core of Internet2, and even suggest improvements in its efficiency, they are not equally effective in detecting other hierarchical modular structures where topological complexity comes from the repetition of a single or finite set of rules. The BA model and the HR network are examples of such repetitive networks. BA shows low Q -modularity and high fractal dimension whereas the Q -modularity and the fractal dimension of HR are moderate and high respectively. Moreover, as we proved, the randomisation processes on these examples always increases the fractal dimension, which measures their topological complexity.

When networks are decomposed into boxes in order to compute their fractal dimension, it is natural to ask for the relationship between the number of interconnections and the box size. We applied Rent’s rule to estimate the interconnection or wiring complexity of the network. Although this power law was initially formulated for VSLI circuits³⁴, a number of authors used Rent’s rule to analyse other biological and technological networks^{22,36,37}. Using the box counting method, we privileged topological aspects against geometrical ones, even if those are certainly interesting. Based on our own method to determine Region II (and also Region III introduced by Stroobandt³⁹), we obtained estimates of Rent’s exponents that slightly differ from those obtained by these authors, but allowed us to draw a reasonable schema: the BA model and the CE connectome have a high wiring complexity, while the other networks have moderate values corresponding to cost-efficient wiring architectures. Moreover, randomisation processes increases Rent’s exponents, a property which was also observed by Reda³⁶ for other biological and technological networks. The HR network shows that a high topological complexity and a moderate wiring complexity are compatible for a network.

Values for Kendall’s coefficient correlating robustness and fixation probability in the non-neutral case $r = 1.5$ with Q -modularity, I -modularity and fractal dimension, see Table 3, suggest a certain correlation with a suitable combination of topological and wiring complexity. However, as we have seen, HR and TW are robust networks with a similar wiring complexity, but a very different topological complexity. The reason for the low fractal dimension of TW resides in its own geometrical construction favouring a sort of spatial aggregation, which is similar to that of a planar lattice. On the contrary, a combination of repetitiveness with some randomness, not present in HR, could justify a gain of topological and wiring complexity without affecting the robustness against invasion of a network like the CE connectome.

Summing up, from the comparison of the *C. elegans* neuronal network with the technological networks PG and I2 and the benchmark models TW and BA emerges the idea of a subtle trade-off between high complexity and low cost. In fact, according to a number of authors^{14,16,17,19,22} and based on their observations, this phenomenon could have been favoured by the evolution. Now, we have a triple challenge: firstly, analyse in more detail the influence of the degree distribution on the robustness, secondly, give a measure of the repetitiveness for networks of any order, and thirdly, quantify its effect on the robustness.

Methods

Robustness. For a homogeneous network G of size N , the Moran process on G reduces to the classical Moran process where all nodes have the same fixation probability

$$\Phi_0(r) = \frac{1 - r^{-1}}{1 - r^{-N}}. \quad (2)$$

Let G be a *weight-balanced network*, that is, the weights of entering edges $w_-(i) = \sum_{j=1}^N w_{ji}$ and leaving edges $w_+(i) = \sum_{j=1}^N w_{ij}$ are equal for any node $i = 1, 2, \dots, N$. Then, according to the Circulation Theorem⁵, the number of elements of each state performs a biased random walk on the integer interval $[0, N]$ with forward bias $r > 1$ and absorbing states 0 and N . Therefore, the fixation probability is the same as that of the homogeneous network of size N . In fact, if G is undirected, the weight of entering edges of a node i can be interpreted as the *temperature* $T_i = \sum_{j=1}^N w_{ji} = \sum_{j \sim i} \frac{1}{d_j}$, where $j \sim i$ means that j is a neighbour of i and d_i is the number of neighbours of i . Hence, an undirected weight-balanced network is *isothermal* because $T_i = T_j$ for all nodes i, j .

On the other hand, the fixation probability of complete bipartite networks $K_{N-m,m}$ converges to the same limit that the fixation probability

$$\Phi_2(r) = \Phi_0(r^2) = \frac{1 - r^{-2}}{1 - r^{-2N}} \quad (3)$$

of the Moran process with fitness r^2 as $N \rightarrow \infty$. In other words, these structures are *evolutionary amplifiers* favouring advantageous invaders.

Let Φ be the fixation function of a network of size N . In order to measure the distance between Φ and Φ_0 , we used the norm $\|\Phi - \Phi_0\|_\infty = \sup_{r \geq 1} |\Phi(r) - \Phi_0(r)|$ and the ratio $\|\Phi - \Phi_0\|_\infty / \|\Phi_2 - \Phi_0\|_\infty$. The *robustness against invasion* of a network is the quotient

$$\rho = \frac{1}{1 + \|\Phi - \Phi_0\|_\infty / \|\Phi_2 - \Phi_0\|_\infty} = \frac{\|\Phi_2 - \Phi_0\|_\infty}{\|\Phi_2 - \Phi_0\|_\infty + \|\Phi - \Phi_0\|_\infty}. \quad (4)$$

Hence, any isothermal network has robustness against invasion 1.

Networks data. The *US Power Grid (PG) network* is the high-voltage power grid in the Western States in the USA¹¹. The nodes are generators, transformers, or substations and the edges are high-voltage transmission lines. Originally used by Watts and Strogatz²⁴, this undirected network has 4,921 nodes and 6,594 edges.

The *Internet2 (I2) network* assembles data from Internet2 community, available now through the Global Research Network Operations Center (GlobalNOC) at Indiana University⁴⁰, which were collected in April 2013. First, we considered the list of active Internet2 Connectors at October 2012. It is an essential part of the Internet2 Combined Infrastructure Topology as described at September 2010. Secondly, we added the list of active Internet2 Primary Participants at April 2013 according to the GlobalNOC website⁴⁰. For more details on the lists of connectors and primary participants, see Supplementary Information. Thus, we obtain a network with 311 nodes and 323 edges. The initial Abilene network (which was replaced by Internet2 in October 2007) was previously analysed by Doyle *et al.*⁴.

The *C. elegans neuronal (CE) network* used here incorporates original data from⁴¹ and updates based upon later work^{42,12}. This version of *C. elegans* connectome has 279 somatic neurones, 6,393 chemical synapses, 890 gap junctions, and 1,410 neuromuscular junctions¹³. According to our aim, we do not distinguish directionality of connections in this network that combines undirected gap junctions with directed chemical synapses, ignoring neuromuscular junctions and synaptic multiplicities. Thus, all the unidirectional connections between two different neurones will be replaced by bidirectional ones leading to a total of 2,290 edges connecting 279 nodes. Since neurones RIBL/R and VA08 have auto-connections, we restrict our attention to 2,287 connections, cf. refs 12,15,22,23. There were efforts on the description of prionic diffusion within the brain⁴³ and the construction of replication models⁴⁴, which are consistent with the Moran process. An analysis of the human brain cluster structure detected by Gallos *et al.*⁴⁵ using fMRI techniques (where modular clusters belong to a region of $N \approx 60,000$ activated voxels) would require additional computational effort.

The *Hierarchical (HR) network* was constructed by Ravasz *et al.*²⁰ as an example of hierarchical modular organisation, see Fig. 5. The one used here has four different levels leading to a total of $4^4 = 256$ nodes and $3 \times (4^3 + 4^2 + 4 + 1) + 4 \times 3 = 267$ edges.

The *Toy Worm (TW) network*²¹ is a random network sampled as follows: it consists of 10^3 networks of order $247 \leq N \leq 256$ which were obtained from a square of 16×16 points in the integer lattice. Let $\phi(x) = e^{-\frac{1}{2}x^2} / \sqrt{2\pi}$ be the density function of the standard normal distribution. Two different nodes u and v in the square are connected by an edge with probability $\phi(d(u, v)) / \phi(0) = e^{-\frac{1}{2}x^2}$ depending on the Euclidian distance $d(u, v)$. The distribution of the number of connected components and the order frequencies of the maximal ones are showed in Supplementary Information. The mean order is $N = 254.74$ with a standard deviation of 1.26.

Finally, the *Barabási-Albert (BA) model* is another random network constructed using the preferential attachment process²⁵. Here, we sampled 10^3 networks of order $N = 200$ starting from $m_0 = 10$ initial nodes and attaching each new node k to $m = 10$ nodes with probability $p_i = 1$ or $p_i = d_i / \sum_{j=1}^{k-1} d_j$ for $1 \leq i \leq k - 1$, depending on whether $k = m_0 + 1$ or $k > m_0 + 1$. We needed 190 iterations to complete each network having 1,900 edges.

Random networks with prescribed degree distribution and fixation probability computation. The problem of generating random networks with a prescribed degree distribution was discussed by many authors^{46–49}. In our case, random network generation was done in NetworkX⁵⁰ using the Markov chain scheme proposed by Gkantsidis *et al.*⁴⁷.

We compared the robustness of the three real networks PG, I2 and CE and the hierarchical deterministic one HR to that of their respective benchmark families of random networks having the same degree distribution. Each

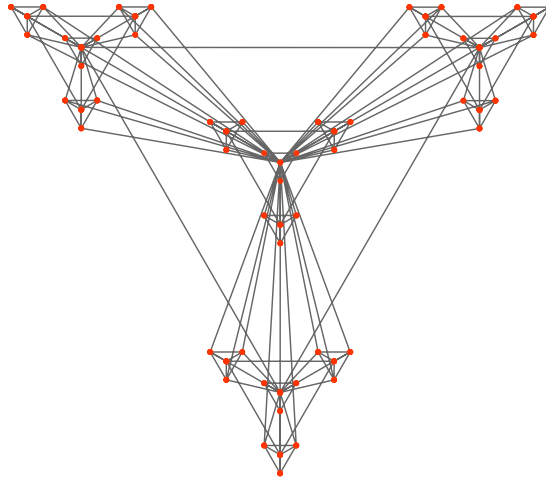


Figure 5. Hierarchical network of level 3 constructed by Ravasz *et al.*²⁰.

family consists of an asymptotically uniform sample of 10^3 networks generated by using the ‘swap’ algorithm⁴⁷, where 10^5 true double-edge swaps were done on each real or deterministic network.

On the other hand, to estimate the average fixation probability for each element of the sample we used the EMC method⁷. We computed the fixation probability function $\Phi(r)$ using sequences of 10^4 trials for each fitness value r varying from 0 to 10 with step size of 0.25 for each of the 10^3 networks in the sample. For the other random networks TW and BA, we did the same simulation from the initial sample of 10^3 networks. The fixation probability function of the original networks PG, I2, CE and HR was computed using 10^5 trials. Finally, we estimated its robustness against invasion (4).

Statistics. We analysed several statistical properties of the four networks PG, I2, CE and HR and their respective randomised benchmarks, as well as those of the two random networks BA and TW. Firstly, for each real or deterministic network, we considered some standard measures such as *mean degree*, *degree median*, *degree variance*, *degree skewness* and *degree kurtosis* related with the degree distribution. We also considered the *heat heterogeneity*¹⁰ defined as the variance of the temperature distribution $H_i = \frac{1}{N} \sum_{i=1}^N (T_i - \bar{T})^2$, where T_i is the temperature of node i and $\bar{T} = \frac{1}{N} \sum_{i=1}^N T_i$ is the mean temperature. As above, for the other random networks, we computed these measures on average from the initial sample of 10^3 networks. Secondly, for any undirected connected network $G = (V, E)$, in addition to the *size* $N = |V|$ and the *edge number* $|E|$, we consider other global measures such as the *diameter* $\Delta = \max_{i,j \in V} d(i, j)$, where $d(i, j)$ is the length of the shortest path between the nodes i and j , and the *temperature entropy*⁸ $I_i = -\frac{1}{N} \sum_{i=1}^N T_i \log(T_i/N)$. Finally, we studied small-world properties of G starting by the *clustering coefficient* $C = \frac{1}{N} \sum_{i=1}^N C_i = \frac{1}{N} \sum_{i=1}^N \frac{2|E_i|}{d_i(d_i-1)}$, where C_i is the density of the induced sub-network $G_i = (V_i, E_i)$ consisting of the set V_i of neighbours of i and the set E_i of edges between neighbours of i . The *transitivity ratio* is a measure of the network transitivity defined as the ratio between the number of nodes in triangles and the triplets of nodes connected by two edges. The *average path length* of G is given by $L = \frac{1}{N(N-1)} \sum_{i \neq j} d(i, j)$. *Power law exponents* were calculated using the *power law* Python package⁵¹ to adequately fit the tail of each degree distribution by a power law with respect to a optimal minimal value d_{\min} .

Rank correlation measures. A rank correlation coefficient is a measure of monotone dependence between two numerical random variables when ranked according to their values. Giving a set $S = \{1, \dots, n\}$ consisting of n individuals, two quantitative properties of these individuals are represented by two vectors $x = (x_1, \dots, x_n)$ and $y = (y_1, \dots, y_n)$. To each pair of individuals i and j , we associate antisymmetric x -score x_{ij} and y -score y_{ij} . A rank correlation coefficient⁵² is defined by

$$\Gamma = \frac{\sum_{i,j=1}^n x_{ij} y_{ij}}{\sqrt{\sum_{i,j=1}^n x_{ij}^2 \sum_{i,j=1}^n y_{ij}^2}}. \quad (5)$$

When x_{ij} is the difference between the ranks of x_j and x_i , *Spearman’s rank correlation coefficient* is obtained. Here, we considered *Kendall’s τ* derived from (5) by choosing

$$x_{ij} = \begin{cases} +1 & \text{if } x_i < x_j, \\ 0 & \text{if } x_i = x_j, \\ -1 & \text{if } x_i > x_j. \end{cases} \quad (6)$$

In our case, each deterministic, random or randomised network is treated as a single network in order to state monotone dependence between two statistics (on average for random or randomised networks). For ordered sets with 10 elements, the upper critical value at a significance level of $p = 0.05$ is $\tau = 0.467$. Statistical computations and graphics were done using the Python scientific stack^{53–56}.

Modularity and hierarchical modularity. A quantity called *Q-modularity*^{28,38} was introduced by Girvan and Newman to measure the decomposability of a network into modules. Given a partition \mathcal{P} of the vertex set $V = \{1, \dots, N\}$ of an undirected connected network $G = (V, E)$, the *modularity of \mathcal{P}* is equal to $Q = \frac{1}{2|E|} \sum_{M \in \mathcal{P}} \sum_{i,j \in M} \left(a_{ij} - \frac{d_i d_j}{2|E|} \right)$, where a_{ij} is the entry of the adjacency matrix corresponding to two nodes i and j in some module $M \in \mathcal{P}$. Several algorithms were proposed to detect the modular structure of the network by finding partitions with the largest value of Q . See a comparative analysis in ref. 38. Recently, methods to study hierarchical modularity were introduced starting from the idea of decomposing modules into submodules, which in turn are decomposed into sub-submodules, and so on. Here, we used the *Louvain method*²⁹, which takes advantage of the hierarchical structure of the network to accelerate the optimisation of Q .

However, as discussed in the comparative analysis by Lancichinetti *et al.*⁵⁷, there are other approaches to identify community structures. We also used the *Infomap* method by Rosvall *et al.*^{30,31}. The modular structure of the network is now achieved by optimising a function, called the *minimum description length I* , which gives account of the balance between information flow and data compression^{30,31}.

Fractal dimension. An alternative definition of modular network was introduced by Song *et al.*^{32,33} representing modules by boxes of different length scales. Any network G admits a decomposition into disjoint *boxes of size b* , i.e. finite sets of nodes of diameter $\leq b - 1$. The fractality of G can be formulated as an invariance property by the renormalisation flow, which replaces each box with a “renormalised” node. The *fractal dimension D* of G can be estimated by two equivalent ways: as the exponent of a power law for the number of boxes of size b

$$N(b) \sim b^{-D}, \quad (7)$$

or as the exponent of a power law for the average number of nodes $N/N(b) \sim b^D$ in a box of size b when b varies from $b = 2$ to the first integer $b \leq \Delta$ such that $N(b) = 1$.

In general, for scale-free networks, it is convenient to use the first method based on power law (7) to find the fractal scaling, although several algorithms can be used to calculate the fractal dimensions, each of them with its pros and cons^{58,59}. Here, we implemented the greedy colouring algorithm proposed by Song *et al.*⁵⁸ according to the description given by Locci *et al.*⁵⁹. The fractal dimension of PG, I2, CE and HR networks was estimated using the ordinary least squares regression on the data gathered from the above algorithm. For each random and randomised network, each of the 10^3 sample elements was partitioned and then D was estimated both computing fractal dimension on average (with the corresponding standard deviations) and fitting a single line to the whole data set. In all cases, standard errors in the fit of the power law (on average in random ones) were also computed and included in Table 2. Naturally, errors decrease as the diameter of network increase. But there is another source of possible error in the estimation of D related with random choices in the construction of the partitions. However, other authors found low values of the standard deviation⁶⁰ which have been corroborate by our own numerical experiments. So we have chosen at random a single partition for each of 10^3 sample elements.

References

- Barabási, A.-L., Jeong, H. & Albert, R. Error and attack tolerance of complex networks. *Nature* **406**, 378–382 (2000).
- Jeong, H., Tombor, B., Albert, R., Oltvai, Z. N. & Barabasi, A.-L. The large-scale organization of metabolic networks. *Nature* **407**, 651–654 (2000).
- Jeong, H., Mason, S. P., Barabasi, A.-L. & Oltvai, Z. N. Lethality and centrality in protein networks. *Nature* **411**, 41–42 (2001).
- Doyle, J. C. *et al.* The “robust yet fragile” nature of the Internet. *PNAS* **102**, 14497–14502 (2005).
- Lieberman, E., Hauert, C. & Nowak, M. A. Evolutionary dynamics on graphs. *Nature* **433**, 312–316 (2005).
- Moran, P. A. P. Random processes in genetics. *Proc. Cambridge Philos. Soc.* **54**, 60–71 (1958).
- Alcalde Cuesta, F., González Sequeiros, P. & Lozano Rojo, A. Fast and asymptotic computation of the fixation probability for Moran processes on graphs. *Biosystems* **129**, 25–35 (2015).
- Voorhees, B. & Murray, A. Fixation probabilities for simple digraphs. *Philos. T. R. Soc. A* **469** (2013).
- Daz, J. *et al.* On the fixation probability of superstars. *Philos. T. R. Soc. A* **469** (2013).
- Tan, S. & Lu, J. Characterizing the effect of population heterogeneity on evolutionary dynamics on complex networks. *Sci. Rep.* **4**, 5034 (2014).
- Koblenz Network Collection. *U.S. Power Grid Network Dataset*. (2015) Available at: <http://konect.uni-koblenz.de>. Accessed: 15/4/2015.
- Varshney, L. R., Chen, B. L., Paniagua, E., Hall, D. H. & Chklovskii, D. B. Structural properties of the *Caenorhabditis elegans* neuronal network. *PLoS Comput. Biol.* **7**, e1001066 (2011).
- Varshney, L. R., Chen, B. L., Paniagua, E., Hall, D. H. & Chklovskii, D. B. *Neuronal connectivity II*. (2015) Available at: <http://www.wormatlas.org/neuronalwiring.html>. Accessed: 15/4/2015.
- Bullmore, E. & Sporns, O. Complex brain networks: graph theoretical analysis of structural and functional systems. *Nat. Rev. Neurosci.* **10**, 186–198 (2009).
- Kim, J. S. & Kaiser, M. From *Caenorhabditis elegans* to the human connectome: a specific modular organization increases metabolic, functional and developmental efficiency. *Philos. T. R. Soc. B* **369**, doi: 10.1098/rstb.2013.0529 (2014).
- Meunier, D., Lambiotte, R. & Bullmore, E. T. Modular and hierarchically modular organization of brain networks. *Front. Neurosci.* **4**, doi: 10.3389/fnins.2010.00200 (2010).
- Meunier, D., Lambiotte, R., Fornito, A., Ersche, K. & Bullmore, E. T. Hierarchical modularity in human brain functional networks. *Front. Neuroinform.* **3**, doi: 10.3389/neuro.11.037 (2009).
- Milo, R. *et al.* Network motifs: Simple building blocks of complex networks. *Science* **298**, 824–827 (2002).
- Sporns, O. Structure and function of complex brain networks. *Dialogues Clin. Neurosci.* **15**, 247–262 (2013).

20. Ravasz, E., Somera, A. L., Mongru, D. A., Oltvai, Z. N. & Barabási, A.-L. Hierarchical organization of modularity in metabolic networks. *Science* **297**, 1551–1555 (2002).
21. Artzy-Randrup, Y., Fleishman, S. J., Ben-Tal, N. & Stone, L. Comment on “Network motifs: Simple building blocks of complex networks” and “Superfamilies of evolved and designed networks”. *Science* **305**, 1107 (2004).
22. Bassett, D. S. *et al.* Efficient physical embedding of topologically complex information processing networks in brains and computer circuits. *PLoS Comput. Biol.* **6**, e1000748 (2010).
23. Pan, R. K., Chatterjee, N. & Sinha, S. Mesoscopic organization reveals the constraints governing *Caenorhabditis elegans* nervous system. *PLoS ONE* **5**, e9240 (2010).
24. Watts, D. J. & Strogatz, S. H. Collective dynamics of ‘small-world’ networks. *Nature* **393**, 440–442 (1998).
25. Barabási, A.-L. & Albert, R. Emergence of scaling in random networks. *Science* **286**, 509–512 (1999).
26. Broom, M., Rychtář, J. & Stadler, B. T. Evolutionary dynamics on small-order graphs. *J. Intesdiscip. Math.* **12**, 129–140 (2009).
27. Broom, M., Rychtář, J. & Stadler, B. T. Evolutionary dynamics on graphs—the effect of graph structure and initial placement on mutant spread. *J. Stat. Theory Pract.* **5**, 369–381 (2011).
28. Newman, M. E. J. & Girvan, M. Finding and evaluating community structure in networks. *Phys. Rev. E* **69**, 026113 (2004).
29. Blondel, V. D., Guillaume, J.-L., Lambiotte, R. & Lefebvre, E. Fast unfolding of communities in large networks. *J. Stat. Mech.-Theory E* **2008**, P10008 (2008).
30. Rosvall, M. & Bergstrom, C. T. Maps of random walks on complex networks reveal community structure. *PNAS* **105**, 1118–1123 (2008).
31. Rosvall, M. & Bergstrom, C. T. Multilevel compression of random walks on networks reveals hierarchical organization in large integrated systems. *PLoS ONE* **6**, e18209 (2011).
32. Song, C., Havlin, S. & Makse, H. A. Self-similarity of complex networks. *Nature* **433**, 392–395 (2005).
33. Song, C., Havlin, S. & Makse, H. A. Origins of fractality in the growth of complex networks. *Nat. Phys.* **2**, 275–281 (2006).
34. Landman, B. & Russo, R. L. On a pin versus block relationship for partitions of logic graphs. *IEEE T. Comput. C-20*, 1469–1479 (1971).
35. Christie, P. & Stroobandt, D. The interpretation and application of Rent’s rule. *IEEE T. VLSI Syst.* **8**, 639–648 (2000).
36. Reda, S. Using circuit structural analysis techniques for networks in systems biology. In *Proceedings of the 11th International Workshop on System Level Interconnect Prediction*, SLIP ’09, 37–44 (ACM, 2009).
37. Partzsch, J. & Schuffny, R. On the routing complexity of neural network models - Rent’s rule revisited. In *ESANN* (2009).
38. Newman, M. E. J. Modularity and community structure in networks. *PNAS* **103**, 8577–8582 (2006).
39. Stroobandt, D. On an efficient method for estimating the interconnection complexity of designs and on the existence of region III in rent’s rule. In *Proceedings of the Ninth Great Lakes Symposium on VLSI*, 330–331 (IEEE, 1999).
40. GlobalNOC. *Internet2 Maps & Documentation*. (2015) Available at: <http://noc.net.internet2.edu/i2network/maps-documentation.html>. Accessed: 3/4/2015.
41. White, J. G., Southgate, E., Thomson, J. N. & Brenner, S. The structure of the nervous system of the nematode *Caenorhabditis elegans*. *Philos. T. R. Soc. B* **314**, 1–340 (1986).
42. Chen, B. L., Hall, D. H. & Chklovskii, D. B. Wiring optimization can relate neuronal structure and function. *PNAS* **103**, 4723–4728 (2006).
43. Hecker, R. *et al.* Replication of distinct scrapie prion isolates is region specific in brains of transgenic mice and hamsters. *Genes. Dev.* **6**, 1213–1228 (1992).
44. Masel, J., Jansen, V. A. & Nowak, M. A. Quantifying the kinetic parameters of prion replication. *Biophys. Chem.* **77**, 139–152 (1999).
45. Gallos, L. K., Sigman, M. & Makse, H. A. The conundrum of functional brain networks: Small-world efficiency or fractal modularity. *Frontiers in Physiology* **3**, 123 (2012).
46. McKay, B. D. & Wormald, N. C. Uniform generation of random regular graphs of moderate degree. *J. Algorithm.* **11**, 52–67 (1990).
47. Gkantsidis, C., Mihail, M. & Zegura, E. The Markov chain simulation method for generating connected power law random graphs. In *In Proc. 5th Workshop on Algorithm Engineering and Experiments (ALENEX03)*, Baltimore, USA. SIAM (2003, January 11).
48. Viger, F. & Latapy, M. Efficient and simple generation of random simple connected graphs with prescribed degree sequence. In *Computing and Combinatorics*, (ed. Wang, L.) vol. 3595 of *Lecture Notes in Computer Science*, 440–449 (Springer, 2005).
49. Bayati, M., Kim, J. & Saberi, A. A sequential algorithm for generating random graphs. *Algorithmica* **58**, 860–910 (2010).
50. Hagberg, A. A., Schult, D. A. & Swart, P. J. Exploring network structure, dynamics, and function using NetworkX. In *Proceedings of the 7th Python in Science Conference (SciPy2008)*, Pasadena, USA (eds Varoquaux, G. *et al.*), 11–15 (2008, August 19). URL http://conference.scipy.org/proceedings/SciPy2008/paper_2/. Accessed: 1/5/2013.
51. Alstott, J., Bullmore, E. & Plenz, D. Powerlaw: A Python package for analysis of heavy-tailed distributions. *PLoS ONE* **9**, e85777 (2014).
52. Kendall, M. *Rank correlation methods* (Charles Griffin & Co. Ltd., 1975), fourth edn.
53. Walt, S. v. d., Colbert, S. C. & Varoquaux, G. The numpy array: A structure for efficient numerical computation. *Computing in Science & Engineering* **13**, 22–30 (2011).
54. McKinney, W. Data structures for statistical computing in python. In *Proceedings of the 9th Python in Science Conference, Austin, USA* (eds van der Walt, S. *et al.*), 51–56 (2010, June 28). URL <http://conference.scipy.org/proceedings/scipy2010/mckinney.html>. Accessed: 10/3/2014.
55. Statsmodels developers. *Statsmodels 0.6.1*. URL <http://statsmodels.sourceforge.net>. Accessed: 1/5/2013.
56. Waskom, M. *et al.* Seaborn: statistical data visualization, *Stanford, California*. doi: 10.5281/zenodo.19108 (2015).
57. Lancichinetti, A. & Fortunato, S. Community detection algorithms: A comparative analysis. *Phys. Rev. E* **80**, 056117 (2009).
58. Song, C., Gallos, L. K., Havlin, S. & Makse, H. A. How to calculate the fractal dimension of a complex network: the box covering algorithm. *J. Stat. Mech.-Theory E* **2007**, P03006 (2007).
59. Locci, M., Concas, G., Tonelli, R. & Turnu, I. Three algorithms for analyzing fractal software networks. *WSEAS Trans. Info. Sci. and App.* **7**, 371–380 (2010).
60. Concas, G., Locci, M. F., Marchesi, M., Pinna, S. & Turnu, I. Fractal dimension in software networks. *EPL* **76**, 1221 (2006).

Acknowledgements

This work was supported by the Spanish Excellence Grant MTM2013-46337-C2-2-P, Galician Grant GPC2015/006 and the European Regional Development Fund. Third author was also supported by the European Social Fund and Government of Aragón (Grant E15), and University of Zaragoza/CUD Grant UZCUD2015-CIE-05.

Author Contributions

F.A., P.G. and Á.L. designed and performed the research as well as wrote the paper.

Additional Information

Supplementary information accompanies this paper at <http://www.nature.com/srep>

Competing financial interests: The authors declare no competing financial interests.

How to cite this article: Alcalde Cuesta, F. *et al.* Exploring the topological sources of robustness against invasion in biological and technological networks. *Sci. Rep.* **6**, 20666; doi: 10.1038/srep20666 (2016).



This work is licensed under a Creative Commons Attribution 4.0 International License. The images or other third party material in this article are included in the article's Creative Commons license, unless indicated otherwise in the credit line; if the material is not included under the Creative Commons license, users will need to obtain permission from the license holder to reproduce the material. To view a copy of this license, visit <http://creativecommons.org/licenses/by/4.0/>